JOURNAL OF CATALYSIS 77, 200–207 (1982)

XPS Study of the Interaction of Oxygen with Nickel Overlayers Deposited on Copper

YASUHIRO MOTOYOSHI, KOSAKU KISHI, AND SHIGERO IKEDA

Department of Chemistry, Faculty of Science, Osaka University, Toyonaka, Osaka 560, Japan

Received December 22, 1981; revised May 6, 1982

The nickel deposited on copper surface was investigated by X-ray photoelectron spectroscopy to show changes in electronic and reaction properties of the nickel. At 0.3 monolayer (ML) coverage the deposited nickel atoms give a Ni $2p_{3/2}$ peak at 852.5 eV, 0.4 eV lower than that of bulk nickel, with no satellite structure. With increasing coverage, the main peak moves to the bulk one and a satellite structure appears as the thick nickel film. The spectral changes are discussed in terms of filling of nickel d-holes by nickel–copper d–d interaction. Reactivity to oxygen of the nickel atoms also changes as a function of coverage. Oxidation of the nickel atoms (to Ni^{2+}) is not observed for the nickel at 0.3 ML coverage after 400 L oxygen exposure. At about 3 ML coverage the nickel overlayers show reactivities comparable to those of thick nickel films. The nickel overlayers (at 0.4 ML) on copper substrate previously exposed to oxygen show a weak but distinct satellite peak with Ni $2p_{3/2}$ peak and are oxidized more easily than those on clean copper. These data indicate an inhibition of nickel–copper interaction by the presence of oxygen ($\theta \simeq 1/3$) on the copper.

1. INTRODUCTION

Structures of monolayer metals deposited on single crystal surfaces of other metals have been studied by using techniques such as low energy electron diffraction (LEED), reflection high energy electron diffraction (RHEED), and transmission electron diffraction (TED), combined with Auger electron spectroscopy (AES) etc. These studies were reviewed by Biberian and Somorjai (*1*). Recently electronic structures of metallic overlayers have been reported with Cu on Zn(0001) (*2*), Cu and Pd on Ag (*3*), Cu on Ni(111) (*4*), Ni on Au, and Au on Ni (*5*) studied by photoelectron spectroscopy. The understanding of the chemistry of metallic overlayers is of basic importance in studies of catalytic reactions, corrosion resistance, and surface segregation of bimetallic alloys and clusters. Reactivity changes have been reported for Pd on Nb(110) (*6*), Au on Pt(100), Pt on Au(100) (*7*), and Cu on Ru (*8–10*). We have reported X-ray photoelectron spectroscopic study of chemically deposited nickel overlayers from $Ni(CO)_4$ on polycrystalline palladium and iron and on the reactivities of these overlayers with oxygen (*11*). The reactivities were correlated with electronic structure changes revealed by the spectral variation of satellite peaks of the Ni $2p_{3/2}$ electrons. In the present paper we report on reactions of oxygen with nickel overlayers, prepared by evaporation, on polycrystalline copper substrates studied by X-ray photoelectron spectroscopy.

2. METHODS

X-Ray photoelectron spectroscopic data were obtained using an AEI ES-200 electron spectrometer with modified sample probe, metal evaporation, and baking arrangements. The base pressure in the sample chamber was $\sim 1 \times 10^{-7}$ Pa. The thick copper substrate films as well as the nickel overlayers were prepared by *in situ* evaporation of the metals under a pressure less than 1×10^{-6} Pa. The copper was evaporated by melting copper wire (0.5 mm in diameter, >99.9% purity) in an electrically heated tungsten wire basket. The tungsten wire was electrolytically cleaned before use by immersing in NaOH aqueous solution

0021-9517/82/090200-08$02.00/0

under a positive potential. A spiral nickel filament (0.6 mm in diameter, >99% purity) was used for the nickel source. Coverages of the nickel overlayers were controlled by rotating the copper plane into and out of the nickel atom flux after evaporation had become steady. The temperature of the sample plate (copper) was maintained at about 300 K during evaporation.

Oxygen gas (99.9% purity) from Takachiho Kagaku Kogyo was passed through a liquid nitrogen trap before use and introduced into the sample chamber in the pressure range 6×10^{-5}–4×10^{-4} Pa. All doses refer to an uncorrected ion gauge reading.

Core electron binding energies, relative to the Fermi level, were determined by referring to a Ni $2p_{3/2}$ value of 852.9 eV for a thick nickel film. In this binding energy scale, the Cu $2p_{3/2}$ peak of the copper substrate was at 932.8 eV.

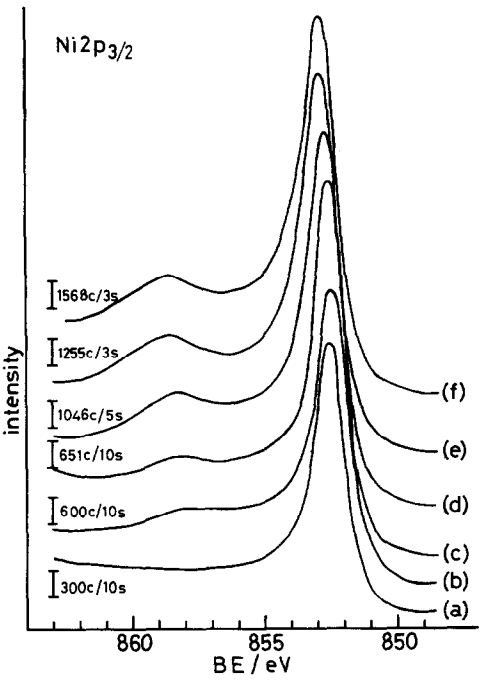

FIG. 1. Ni $2p_{3/2}$ spectral region for various coverages of nickel deposited on polycrystalline copper surface: (a) 0.3 ML, (b) 0.7 ML, (c) 1.0 ML, (d) 2.4 ML, and (e) 7.9 ML, and for (f) thick nickel film.

3. RESULTS AND DISCUSSION

3.1. Deposition of Nickel on Copper

Figure 1 shows the Ni $2p_{3/2}$ spectral region for the nickel deposited on copper film (curves a to e) as a function of the coverage of the overlayers and for the thick nickel film (f). The coverages were estimated both from the Ni $2p_{3/2}$ intensity (by height) and from attenuation of Cu $2p_{3/2}$ or Cu $L_3M_{4,5}$ $M_{4,5}$ Auger peak intensity. In each experiment, the Cu $2p_{3/2}$ peak of thick copper substrate before nickel evaporation was used as calibration standards for the intensity measurements. The following equations were used for the estimation of the coverages on assuming uniform thicknesses, d, for the overlayers.

$$d = -\lambda_a \cdot \sin\theta \cdot \ln(1 - I_a/I_a^\circ)$$

or

$$d = -\lambda_s \cdot \sin\theta \cdot \ln(I_s/I_s^\circ)$$

where $I_a^\circ$and $I_s^\circ$are the peak intensities from thick nickel and copper films, I_a and I_s the intensities from nickel overlayers and the copper substrate after nickel evaporation, respectively, and θ is an electron collection angle with respect to the sample plane (60° in this experiment). Electron mean free path values, λ_s for the copper peaks and λ_a for the nickel peak, in the overlayers were calculated from an equation presented by Seah and Dench (*12*). The values are 1.27 nm for Ni $2p_{3/2}$ (kinetic energy ~630 eV), 1.19 nm for Cu $2p_{3/2}$ (~550 eV), and 1.53 nm for Cu $L_3M_{4,5}$ $M_{4,5}$ Auger electrons (~910 eV). The overlayer coverages expressed in monolayer (ML) unit were obtained simply by d/0.25 nm (approximate monolayer thickness). The real thickness seems to be slightly larger than the estimated values when the overlayers were formed by crystallite growth mechanism, multiple-atom height growth.

In Fig. 2, the overlayer coverages obtained from Ni $2p_{3/2}$ intensity are compared with those from Cu $2p_{3/2}$ and Cu Auger intensities. In the region less than about 2 ML, the coverage estimated from Ni $2p_{3/2}$

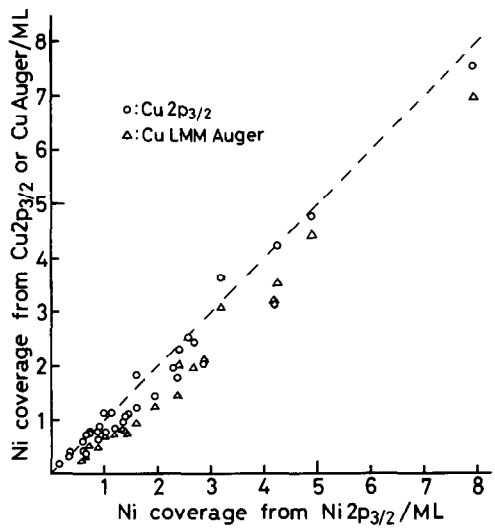

FIG. 2. The relation between the nickel overlayer coverage estimated from Ni $2p_{3/2}$ and that from Cu $2p_{3/2}$ or Cu LMM Auger electron (○, Ni $2p_{3/2}$ vs Cu $2p_{3/2}$; △, Ni $2p_{3/2}$ vs Cu LMM Auger).

intensity gave errors arising from use of peak height for the intensity. A maximum error was about 30% overestimation at 0.3 ML. The coverages from the peak height were, however, plotted since the exact estimation from the peak areas including satellite peaks was not easy because of difficulty in background evaluation. The values obtained from Ni $2p_{3/2}$ peaks are slightly larger than the values from Cu peaks in the region above 2.4 ML. The difference may be explained by multiple-atom-height island growth.

As shown in Fig. 1, the main Ni $2p_{3/2}$ peak at 852.9 eV for thick nickel film (curve f) shifted to lower binding energy with decreasing overlayer coverage (from e to a). Figure 3 shows the shifts as a function of coverage. The shifts are nearly constant, ~ -0.35 eV, up to about 0.8 ML and increase to the bulk value at 10 ML. The shifts, -0.35 eV, is smaller than that observed for Ni on Au, -0.8 eV (*5*). In the case of Ni on Au, the shifts change with variation of the mean Ni–Ni nearest neighbor coordination number with increasing overlayer coverages. The shifts for Ni on Cu are interpreted presumably in terms of the same variation of the Ni–Ni coordination number.

The satellite feature of the Ni $2p_{3/2}$ peak also varied in intensity and energy with increasing overlayer coverages as in Fig. 1. At 0.3 ML, no satellite peak was found (curve a). A small satellite was observed at 0.7 ML (b). The satellite obtained at 2.4 ML (d) showed the same intensity as the thick nickel film (f). The satellite to main peak distance changed with coverage as follows: 5.5 eV (1.0 ML), 5.7 eV (2.4 ML), 5.8 eV (7.9 ML), and 5.9 eV (thick nickel film). Similar spectral variations of the satellite have been reported for Ni on Pd (*11*), Ni on Au (*5*), and for alloys of Ni–Pd (*11*), Ni–Au (*16*), and Ni–Th (*17*). The satellite peak of metallic nickel has been suggested to be due to shake-up processes (*18–20*) and excitation of electron-hole pairs in the conduction d-bands in the presence of a photoelectron induced hole (*21–23*). The decrease in the satellite intensity for ThNi alloys has been related to a reduction in the d-hole density arising from filling of nickel d-holes by adjacent electropositive thorium. The energy separating the satellite and the main peak increased in going from Ni (5.9 eV) to ThNi (~7.2 eV). Similar effects have been discussed in reference to Auger spectra in unfilled d-band metals (*24*). The spectral changes on the satellite for Ni on Cu at present study also appear to be related to the changes in electronic states of the nickel valence electrons due to nickel–copper interaction.

In case of Cu on Ni(111) where the charge transfer was considered to be small between the adatoms and the substrate, the electronic states of Cu adatoms have been

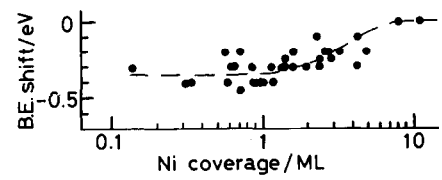

FIG. 3. Ni $2p_{3/2}$ peak shift as a function of nickel coverage.

concluded by UPS data to depend strongly upon a d–d interaction between the adatoms and the substrate (*4*). The local density of states calculation has shown the importance of the d–d interaction. Similar d–d interaction is expected for the reversed system, Ni on Cu. The nickel atoms on copper showed decrease in the satellite intensity with decreasing nickel coverages and the main nickel peak became less asymmetric (Fig. 1a). The decrease in the satellite intensity can be related to the decrease in d-holes as in case of Th–Ni alloys. However, the energy separating the satellite and the main peak decreased a little, ~0.4 eV, with decreasing satellite intensity while the corresponding energy separation increased in going from Ni to ThNi alloy by ~1.3 eV. This seems to indicate that a mechanism for reduction in the d-holes of nickel on copper is somewhat different from the filling of the d-holes by charge transfer from copper. The charge transfer to nickel from copper should be considerably smaller than from electropositive thorium. Another possible mechanism is a redistribution of valence electrons between d and sp bands in nickel atoms during the nickel–copper interaction.

The energy separation decreased considerably in nickel overlayers deposited from $Ni(CO)_4$ on palladium with decreasing coverage (4.3 eV separation at 0.12 ML and 4.8 eV at 0.42 ML) and the satellite became an asymmetric tail of the main peak without losing its intensity (*11*). The same changes were observed for the nickel overlayers obtained by evaporation of nickel onto palladium (*25*). According to the mechanism described above for the spectral changes in unfilled d-band metals (*21–24*), the decrease in the energy separation can be interpreted by the increase in nickel d-holes, namely, a charge transfer to adjacent palladium atoms from nickel. This reveals that the electronic states of Ni on Cu are considerably different from those of Ni on Pd. These data show that the spectral changes on the satellite originate rather from the adatom–substrate interaction than from a very small thickness or size of the nickel.

3.2. Interaction with Oxygen

In the previous paper (*11*) has been reported the reactivity change of nickel adatoms on palladium with oxygen depending on the nickel overlayer coverages. The nickel–copper d–d interaction, followed by the electronic change in the nickel adatoms as discussed above, should also be reflected in the reactivities of the nickel to oxygen as on the Ni on Pd. Figure 4 shows the Ni $2p_{3/2}$ spectral region before and after oxygen exposure to the nickel overlayers on copper (curves a to d) and to thick nickel film (e). The overlayer coverages were estimated as 0.3 ML (curves a), 1.0 ML (b), 2.4 ML (c), and 7.9 ML (d), respectively. In every case (a to e), the three curves correspond to the spectra obtained for (i) clean surfaces and the surfaces after (ii) 100 L and (iii) further 300 L oxygen exposure. At 0.3 ML coverage, the Ni $2p_{3/2}$ peak with no satellite showed a little (<15%) attenuation and a slight broadening after 400 L oxygen exposure but no shift in binding energy (a–iii). If the nickel adatoms have the same reactivity to oxygen as thick nickel film which forms 3 NiO layers (*26, 27*) under similar conditions, the adatoms must be oxidized completely to show a large shift in the Ni $2p_{3/2}$ peak. The lack of the shift for the nickel at 0.3 ML reveals that nearly all of the adatoms was not oxidized to Ni^{2+} after 400 L oxygen exposure since even isolated nickel atoms (~0.1 ML) on amorphous carbon showed a large shift after exposure to air at an atmospheric pressure (*28*). The very little oxidation of the adatoms is considered to arise mainly from the nickel–copper interaction discussed above and a resultant electronic change in the nickel atoms leading to nickel–copper and nickel–nickel bonds which are not broken by oxygen. The nickel atoms can chemisorb oxygen as discussed below concerning O 1s peaks.

At 1.0 ML coverage, the Ni $2p_{3/2}$ inten-

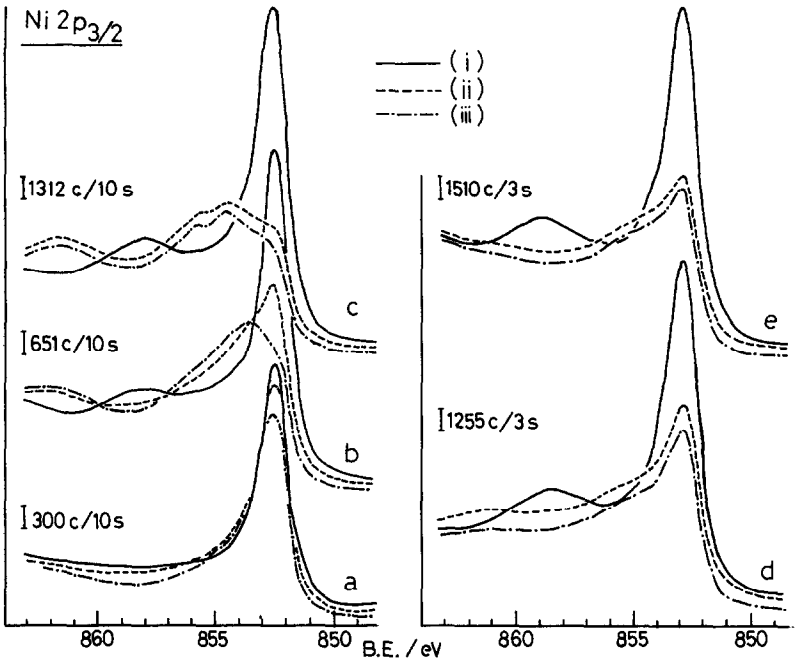

FIG. 4. Ni $2p_{3/2}$ spectral region for deposited nickel: (a) 0.3 ML, (b) 1.0 ML, (c) 2.4 ML, and (d) 7.9 ML, and (e) for thick nickel film [(i) before oxygen exposure, (ii) after 100 L oxygen exposure, and (iii) subsequent 300 L oxygen exposure].

sity at 852.5 eV was attenuated by 40% after 100 L oxygen exposure (curve b–ii) and broad tailing was observed on higher binding energy side. Additional 300 L oxygen exposure depressed the Ni $2p_{3/2}$ peak further at 852.5 eV and gave a new peak at 853.7 eV (b–ii). The binding energy, 853.7 eV, is smaller than that for the NiO layers, ~854.7 eV, formed by exposing nickel surface to oxygen at 295 K (*26*), suggesting formation of a nickel oxide whose nickel ions are surrounded by less oxygen ions than in bulk NiO. A broad shoulder appeared around 862 eV. On the palladium substrate, the nickel overlayers at 1 ML showed much lower reactivity to oxygen than those on copper; after 900 L oxygen exposure, the prominent Ni $2p_{3/2}$ peak was the metallic one at 852.9 eV and the oxide peak was observed only as a shoulder around 855 eV. The electron transfer from nickel to palladium, as suggested in Section 3.1, may account for the lower reactivity to oxygen of the nickel on palladium than on copper.

At 2.4 ML coverage the metallic Ni $2p_{3/2}$ peak at 852.6 eV was attenuated by >65% after 100 L oxygen exposure (curve c–ii). The other Ni $2p_{3/2}$ peaks appeared at 854.6, 856.0, and 861.5 eV. Further, 300 L, oxygen exposure gave no significant change in the spectra (c–iii). The peaks at 854.6, 856.0, and 861.5 eV correspond well to those at 854.7, 856.8, and 861.8 eV observed for thick NiO grown by exposing a Ni(111) surface to oxygen at 1300 K (*26*), indicating the formation of NiO layers. The remaining metallic peak at 852.6 eV implies that the nickel atoms bonding directly to copper substrate were not oxidized. At 7.9 ML coverage, the oxide peaks were observed only as shoulders (curve d–iii) as well as for thick nickel film (e–iii). The nickel atoms of 8 ML coverage can give the Ni $2p_{3/2}$ intensity of about 84% of that for thick nickel film and therefore exhibit spec-

tral changes of the Ni $2p_{3/2}$, during oxygen exposure, which are similar to those observed for thick nickel film. The very broad Ni $2p_{3/2}$ peak profile of the oxide (due to Ni^{2+}) makes the peak indistinct compared to that for the metallic peak in spite of substantial (about 50%) attenuation of the metallic peak.

Reactivity changes due to adatoms–substrate interaction have been reported for several systems (*6–11*). Shi *et al.* found the strong inhibition in the reaction of Ru substrate to N_2O by deposition of very small amounts of Cu as an overlayer on Ru (*8*). They also pointed out that surfaces with less than three monolayers of Cu exhibited higher dissociation probabilities of N_2O and larger sticking coefficients of O_2 than bulk copper. Ertl *et al.* have reported on studies of the interaction of hydrogen (*9*) and carbon monoxide (*10*) on Cu-covered Ru(0001). Sachtler *et al.* have reported a reactivity change on the Pt-deposited Au(100) and Au-deposited Pt(100) surfaces using cyclohexene dehydrogenation to benzene (*7*). A shift of charge density has been proposed as one of the possible causes for the observed reactivity enhancement of a Pt(100) single crystal surfaces by gold. The importance of the electronic change was shown also in our studies for the reactivity of nickel adatoms on iron, palladium (*11*), and copper although the structural change is another significant factor. The satellite features and asymmetric line shapes for the Ni $2p_{3/2}$ signals can be used as a probe for the electronic states and reactivities of the nickel adatoms.

At low (<1.5 ML) nickel coverages, the O 1s intensities, namely, oxygen uptake, were small after 100 L oxygen exposure. Subsequent 300 L exposure enhances considerably the O 1s intensity. At higher (>2 ML) nickel coverage, O 1s peaks after 100 L exposure showed virtually no increase in intensity during further, 300 L, exposure. These results also demonstrate the lower reactivity to oxygen of the nickel adatoms at low coverages and/or lower probabilities

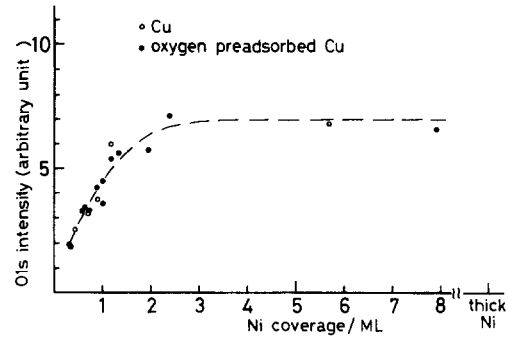

FIG. 5. O 1s spectral intensity after 400 L oxygen exposure as a function of nickel overlayer coverage (●, nickel deposited on copper; ○, nickel deposited on oxygen preadsorbed copper).

of oxygen penetration. In Fig. 5 is shown the variation of the O 1s intensity after (100 L + 300 L) oxygen exposure as a function of nickel coverage. The intensities increase linearly up to ~1.2 ML. The O 1s binding energies shifted from 529.9 eV for ~0.3 ML nickel to 529.6 eV for ~1 ML nickel. Similar O 1s shifts were observed in the reaction of oxygen with Ni(100) and Ni(110) surfaces at 295 K with increasing oxygen coverage, θ (*26*). The O 1s peak located at ~530.4 eV at $\theta < 0.3$ and decreased continuously in energy at $0.3 < \theta \lesssim 0.6$, finally reaching a value of 529.7 eV, characteristic of bulk NiO, during oxide nucleation and growth. The higher binding energy of the O 1s peak at 529.9 eV suggests that oxygen chemisorbs on the surface of 0.3 ML nickel layers on copper. This is supported by the fact that the nickel adatoms at 0.3 ML, after 400 L oxygen exposure, showed no Ni $2p_{3/2}$ peak which was associated with Ni^{2+}. The O 1s peak at 529.6 eV for the nickel overlayers at ~1 ML reveals a commencement of the NiO lattice formation, oxygen-deficient oxide formation, as proposed by the Ni $2p_{3/2}$ binding energy. The gradual increase in the O 1s intensity in the coverage region, ~1.2 ML to ~3 ML, shows the oxide growth. The intensity saturates at ~3 ML. The saturation intensity is about 70% of that obtained for the thick nickel film. The difference may be due to the different surface roughness.

3.3. *Deposition of Nickel on Oxygen-Preadsorbed Copper*

Nickel was deposited on a copper substrate which had been previously exposed to oxygen (300 L) in order to get further information about the effect of the nickel–copper interaction on the reactivity to oxygen of the nickel overlayers. Oxygen coverage on the copper substrate before nickel evaporation was estimated to be about 1/3 from the O 1s intensity. In Fig. 6 are shown the Ni $2p_{3/2}$ spectral region before and after oxygen exposure to the nickel overlayers (curves a to d). The estimated coverages of the overlayers were 0.4 ML (curves a), 0.9 ML (b), 1.2 ML (c), and 5.7 ML (d), respectively. In every case (a to d) the three curves correspond to the spectra obtained (i) before oxygen exposure to the surface, (ii) after 100 L, and (iii) further 300 L oxygen exposure. In case of 0.4 ML coverage, the nickel overlayer gave the Ni $2p_{3/2}$ peak at 852.6 eV and a small, but distinct, satellite peak around 858 eV (a–i). This means that the nickel adatoms on the oxygen preadsorbed copper were in a different electronic state from those at 0.3 ML on the clean copper which gave no satellite peak. After 100 L oxygen exposure the main peak was attenuated by 19% (a–ii). Further, 300 L, oxygen exposure shifted the main peak to 853.5 eV with broadening (a–iii), showing a formation of the oxygen-deficient NiO as discussed in Section 3.2. The Ni $2p_{3/2}$ spectral features after oxygen exposure (a–iii) were quite similar to those observed for the nickel overlayer of 0.7 ML on the clean copper substrate. The nickel adatoms (at 0.9 ML) on oxygen-precovered copper were readily oxidized, after 400 L oxygen exposure, to form an NiO-like compound, which gave the Ni $2p_{3/2}$ peak around 854 and 856 eV (b–iii), in contrast to the formation of oxygen-deficient oxide for the nickel (at 1.0 ML) on the clean copper (Fig. 4b–iii). As shown by curve c–ii in Fig. 6, 100 L oxygen exposure was enough for the nickel at 1.2 ML to give the Ni $2p_{3/2}$ peaks at 854.3 and 856.0 eV due to NiO-like com-

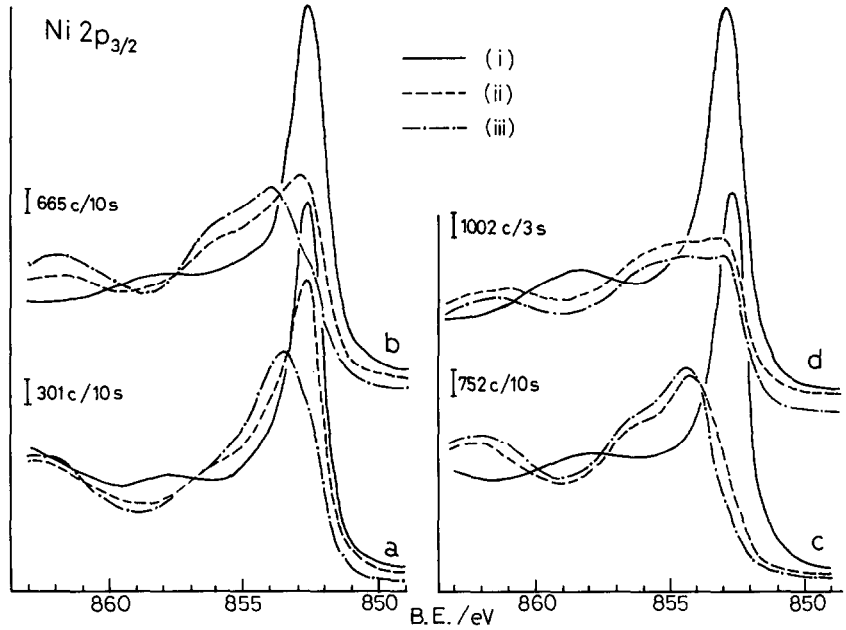

FIG. 6. Ni $2p_{3/2}$ spectral region for nickel deposited on copper pretreated with 300 L oxygen: (a) 0.4 ML, (b) 0.9 ML, (c) 1.2 ML, and (d) 5.7 ML [(i) before oxygen exposure, (ii) after 100 L oxygen exposure, and (iii) after subsequent 300 L oxygen exposure].

pound. Further 300 L exposure gave no significant change in the spectra (c–iii). At 5.7 ML, the overlayer nickel was easily oxidized after 100 L oxygen exposure (d–ii). The presence of a clear metallic peak at 852.9 eV indicates an increase in the unoxidized nickel under the NiO layers. The above results lead to the conclusion that the nickel overlayers at small coverage were more easily oxidized on the oxygen-precovered copper substrate than those on the clean copper. This is ascribable to the fact that the preadsorbed oxygen (about 33% coverage) on copper partly blocked the nickel–copper interaction which would bring about the change in electronic states of the adatoms.

4. CONCLUSIONS

The XPS Ni $2p_{3/2}$ peak of nickel deposited on copper substrate differs in peak position and satellite splitting from that of a thick nickel film. The main peak at 852.9 eV for the thick nickel film shifted to lower binding energy with decreasing overlayer coverages: ~ -0.35 eV shift at 0.8 ML coverage. The shifts are interpreted in terms of the variation of the Ni–Ni coordination number. The nickel overlayers at 2.4 ML gives the same intensity of the satellite as the thick nickel film but the nickel adatoms at 0.3 ML show no satellite peak. This can be related to the adatom–substrate d–d interaction and a resultant decrease in d-holes of the nickel.

The nickel overlayers at small coverages show lower reactivity to oxygen than the thick nickel film. This likely arose mainly from the nickel–copper interaction leading to the change in electronic states of the nickel atoms and to the nickel–copper and nickel–nickel bonds which are not broken by oxygen.

The preadsorbed oxygen (about 33% coverage) on the copper substrate interrupts the nickel–copper interaction and consequently the nickel overlayers on the surface are easily oxidized even at small coverages.

REFERENCES

1. Biberian, J. P., and Somorjai, G. A., *J. Vac. Sci. Technol.* **16,** 2073 (1979).
2. Abbati, I., Braicovich, L., Bertoni, C. M., Calandra, C., and Manghi, F., *Phys. Rev. Lett.* **40,** 469 (1978).
3. Eastman, D. E., and Grobman, W. D., *Phys. Rev. Lett.* **30,** 177 (1973).
4. Abbati, I., Braicovich, L., Fasana, A., Bertoni, C. M., Manghi, F., and Calandra, C., *Phys. Rev. B* **23,** 6448 (1981).
5. Steiner, P., and Hüfner, S., *Solid State Commun.* **37,** 279 (1981).
6. El-Batanouny, M., Strongin, M., Williams, G. P., and Colbert, J., *Phys. Rev. Lett.* **46,** 269 (1981).
7. Sachtler, J. W. A., Biberian, J. P., and Somorjai, G. A., *Surf. Sci.* **110,** 43 (1981).
8. Shi, S.-K., Lee, H.-I., and White, J. M., *Surf. Sci.* **102,** 56 (1981).
9. Shimizu, H., Christmann, K., and Ertl, G., *J. Catal.* **61,** 412 (1980).
10. Vickerman, J. C., Christmann, K., and Ertl, G., *J. Catal.* **71,** 175 (1981).
11. Kishi, K., Motoyoshi, Y., and Ikeda, S., *Surf. Sci.* **105,** 313 (1981).
12. Seah, M. P., and Dench, W. A., *Surf. Interface Anal.* **1,** 2 (1979).
13. Citrin, P. H., Wertheim, G. K., and Baer, Y., *Phys. Rev. Lett.* **41,** 1425 (1978).
14. Duc, T. M., Guillot, C., Lassailly, Y., Lecante, J., Jugnet, Y., and Vedrine, C., *Phys. Rev. Lett.* **43,** 789 (1979).
15. van der Veen, J. F., Himpsel, F. J., and Eastman, D. E., *Phys. Rev. Lett.* **44,** 189 (1980).
16. Höchst, H., Steiner, P., and Hüfner, S., *Z. Phys. B* **38,** 201 (1980).
17. Fuggle, J. C., and Zolnierek, Z., *Solid State Commun.* **38,** 799 (1981).
18. Tibbets, G. G., and Egelhoff, W. F., Jr., *Phys. Rev. Lett.* **41,** 188 (1978).
19. Andrews, P. T., Collins, T., Johnson, C. E., and Weightman, P., *J. Electron Spectrosc.* **15,** 39 (1979).
20. Gibbs, R. A., Winograd, N., and Young, V. Y., *J. Chem. Phys.* **72,** 4799 (1980).
21. Hüfner, S., and Wertheim, G. K., *Phys. Lett.* **51A,** 299 (1975).
22. Tersoff, J., Falicov, L. M., and Penn, D. R., *Solid State Commun.* **32,** 1045 (1979).
23. Mårtensson, N., and Johansson, B., *Phys. Rev. Lett.* **45,** 482 (1980).
24. Tréglia, G., Desjonquères, M. C., Duncastelle, F., and Spanjaard, D., *J. Phys.* **C14,** 4347 (1981).
25. Kishi, K., and Ikeda, S., unpublished data.
26. Norton, P. R., Tapping, R. L., and Goodale, J. W., *Surf. Sci.* **65,** 13 (1977).
27. Rieder, K. H., *Appl. Surf. Sci.* **2,** 74 (1978).
28. Egelhoff, W. F., Jr., and Tibbetts, G. G., *Phys. Rev.* **B19,** 5028 (1979).